Partially Structured Self-Associating States of Acidic Fibroblast Growth Factor

Henryk Mach, James A. Ryan, Carl J. Burke, David B. Volkin, and C. Russell Middaugh*

Department of Pharmaceutical Research, Merck Research Laboratories, WP78-302, West Point, Pennsylvania 19486

Received April 12, 1993; Revised Manuscript Received May 24, 1993

ABSTRACT: A combination of near- and far-UV circular dichroism, Fourier-transform infrared spectroscopy, tryptophan fluorescence, size-exclusion chromatography, and a fluorescent extrinsic hydrophobic probe has been employed to characterize partially structured states of human recombinant acidic fibroblast growth factor (aFGF). At low pH, the addition of specific polyanionic ligands or moderate amounts of salts induces states with high secondary but low tertiary structure content. At neutral pH, intermediate amounts of chaotropic agents impose similar partially structured conformational states which also display noncooperative unfolding transitions. Kinetic evidence indicates that similar forms of the protein exist in the first few hundred milliseconds in the refolding pathway of aFGF. The kinetics of their formation appear to be temperature-independent, implying lack of an energy barrier, which is characteristic for further slow folding into the native state. Unlike the native and fully unfolded states, these partially structured conformations exhibit very low solubility, resulting in irreversible aggregation. Potential physiological implications of the existence of such "molten globule" states with regard to the growth factor's transport and biological activity are considered.

Recent work has suggested that many if not most proteins collapse to a relatively compact form early in their *in vitro* folding pathways. Similar states appear to also exist under equilibrium conditions at low pH and high anion concentration as well as under moderate structure-perturbing conditions [reviewed by Kuwajima (1989), Baldwin (1991), Christensen and Pain (1991), and Dobson (1992)]. These nonnative conformations share the properties of extensive secondary structure, minimal tertiary interactions (e.g., extensive solvent exposure of previously buried apolar moieties), and a tendency to aggregate. Such states are also characterized by an ability to bind hydrophobic dyes [e.g., 8-anilino-1-naphthalenesulfonate (ANS)][1] and noncooperative unfolding transitions. Such compact, partially structured conformations are usually collectively referred to as "molten globules" (MG) and will be so designated herein without further use of quotation marks. This term as used throughout these investigations is not intended in any prejudicial manner but is merely used to refer to the ill-defined collection of conformational states described above.

Acidic fibroblast growth factor (aFGF) is a 16-kDa protein possessing mitogenic, angiogenic, and chemotactic stimulatory activities [reviewed by Burgess and Maciag (1989)]. The three-dimensional structure of the bovine form of the protein has been determined by X-ray crystallography and has been found to consist of 12 antiparallel β strands oriented with pseudo 3-fold symmetry (Zhu et al., 1991). The protein displays a strong dependence on the presence of a polyanion such as heparin for both its stability and its biological activity (Gospodarowicz & Cheng, 1986) and is actually significantly unfolded in the absence of such a stabilizing ligand at physiological temperatures (T >30 °C) (Copeland et al., 1991). Unfolded aFGF can, however, be induced to refold at higher temperatures in the presence of a variety of polyanions. Interestingly, polyanions have little effect on the rate of refolding of aFGF between 5 and 30 °C, but different polyanions produce quite different activation energies of refolding at temperatures from 30 to 50 °C (Dabora et al., 1991). Thus, the rate of refolding of aFGF at T >30 °C appears to be controlled by the interaction of a nativelike state of the protein with polyanions. The rate of refolding is not influenced by the presence of a molecular chaperone (hsp70) or a peptidylprolyl isomerase (FKBP) (Dabora et al., 1991). These observations suggest that the early folding events of aFGF might involve some sort of compact, MG-like state. Previous studies of these states have focused on primarily helical proteins [see Baldwin (1991)], quite different than this β-structure-rich growth factor. Furthermore, aFGF possesses unique spectroscopic properties (Copeland et al., 1991) that make it particularly attractive as the subject of study of its nonnative conformational states. In this work, we describe the presence of equilibrium MG states in aFGF and present evidence that related states occur early in the protein's refolding pathway. Furthermore, we demonstrate that such states are induced and stabilized by polyanions that also bind to the native form of the protein and that aggregation of aFGF under various conditions appears to be preceded by formation of MG states.

MATERIALS AND METHODS

Recombinant human acidic fibroblast growth factor was prepared from transformed *Escherichia coli* as described previously (Linemeyer et al., 1987; Copeland et al., 1991). The 141 amino acid form of the protein employed in these studies lacks the first 13 residues of the natural form but has similar mitogenic activity, receptor binding, heparin dependence, and spectroscopic properties (Volkin et al., 1993). The purity of the growth factor was >99% as assessed by SDS–PAGE using silver staining. Protein concentration was determined spectrophotometrically with a Hewlett-Packard 8450A spectrophotometer employing an extinction coefficient at 280 nm ($E^{0.1\%}_{1cm}$) of 1.2. Bovine lung heparin (average MW = 16K) was purchased from Hepar (Franklin, OH).

* To whom correspondence should be addressed. Telephone: (215) 652-3438. FAX: (215) 652-5299.

[1] Abbreviations: ANS, 8-anilino-1-naphthalenesulfonate; MG, molten globule(s); aFGF, acidic fibroblast growth factor; SDS–PAGE, sodium dodecyl sulfate–polyacrylamide gel electrophoresis; EDTA, ethylenediaminetetraacetic acid; FTIR, Fourier transform infrared spectroscopy; CD, circular dichroism; SEC, size-exclusion chromatography; hsp70, heat shock protein 70; FKBP, FK-506 binding protein.

0006-2960/93/0432-7703$04.00/0

Lithium perchlorate (ACS grade) was obtained from Aldrich (Milwaukee, WI). Other chemicals were obtained from Sigma (St. Louis, MO) and were used as received. A buffer containing 10 mM sodium phosphate and 0.1 mM EDTA (supplemented with 1 mM DTT when indicated) was used throughout this study. Adjustment of pH was performed with either 1 or 11.4 N HCl. Ultraviolet absorbance, fluorescence, FTIR and CD spectra were acquired at 20 °C except in refolding experiments where a 3–23 °C range was employed.

Circular Dichroism. Steady-state and kinetic CD measurements were performed with either an AVIV 62DS or a Jasco J-720 spectropolarimeter calibrated with camphorsulfonic acid. A protein concentration of approximately 0.1 mg/mL and 1-mm cells were employed for far-UV measurements and 10-mm cells with 1 mg/mL protein concentrations for near-UV CD studies. At least three spectra were acquired and averaged for each sample. Time-dependent changes in far-UV CD spectra after dilution from 3.0 to 0.6 N $LiClO_4$ were monitored by measuring spectra from 200 to 240 nm every 30 s, employing a 10-nm bandwidth. Protein concentrations were determined before and after each experiment from UV absorbance spectra. To maintain optical transparency in the far-UV region, lithium perchlorate was employed as a structure-perturbing agent.

Fourier Transform Infrared Spectroscopy. Infrared spectra were recorded at 2-cm^{-1} resolution in 0.1-mm CaF_2 cells with a Digilab FTS60 FTIR spectrometer equipped with a mercury–cadmium–telluride detector. A 1-mL aliquot of aFGF solution (approximately 0.5 mg/mL) supplemented with specific anions at the indicated concentrations was dialyzed against deuterium oxide buffers of identical composition, employing a 5-well microdialysis system (Pierce, Rockford, IL). The completeness of H_2O/D_2O exchange was verified by disappearance of the amide II band. Spectra were collected at room temperature. Initially, spectra were deconvoluted by the method of Kauppinen et al. (1981) employing an enhancement factor (K) of 1.5 and a bandwidth at half-height (σ) of 16. These partially deconvoluted spectra were fit to a series of Gaussian/Lorentzian mixed peaks using peak positions from second-derivative spectra as initial estimates. Assignments were based on the studies of Byler and Susi (1986) as previously described (Copeland et al., 1991).

Fluorescence Spectroscopy. Steady-state and kinetic fluorescence measurements were performed with a Hitachi F-2000 spectrofluorometer interfaced to a personal computer. Spectra-Calc software (Galactic Industries) was employed to control the instrument and perform calculations. Steady-state spectra were acquired with 10-nm excitation and emission bandwidths. An excitation wavelength of 270 nm was employed for excitation of both Tyr and Trp residues and 370 nm to induce ANS emission. Kinetic measurements were performed by acquiring consecutive spectra employing a rapid scanning speed of 1200 nm/min. The positions of the Trp and ANS fluorescence maxima were determined by calculation of first-derivative spectra using 2-nm intervals and 10 data-point windows (Savitzky & Golay, 1963; Steiner et al., 1967). The intersections of these derivative curves with the abscissa yielded peak positions. In urea denaturation experiments, an equilibrium constant K describing the reversible conversion between MG and more completely unfolded states was calculated for each urea concentration employed:

$$K = \frac{F_N - F}{F - F_D}$$

where F_N, F_D, and F are values of the normalized fluorescence intensity at 340 nm or the emission maximum wavelength (λ_{max}) of MG (no urea), unfolded (6 M urea), and intermediate states (0–6 M urea, 0.125 M increments), respectively. The method by which thermodynamic parameters were calculated is described in Table I. Samples were incubated at 20 °C for 1 h prior to analysis, since longer incubation times did not further alter fluorescence intensity ratios.

Stopped-flow fluorescence measurements were performed with an OLIS-3000 apparatus possessing a mixing dead time of <3 ms and a 1:1 mixing volume ratio. To monitor ANS fluorescence, excitation was set at 320 nm and emission intensity monitored through a 348-nm cut-off filter. Two hundred data points were obtained in each experiment, and the consistency of the results was tested by performing at least three repetitions. No signal change was observed upon mixing of preformed MG states with the buffer used to induce this state.

Size-Exclusion Chromatography. Gel filtration studies were performed using a protein concentration of 0.05 mg/mL at 25 °C with a Toso-Haas G3000 SW_{XL} column (0.78 × 30 cm) and a Rainin Rabbit HPLC system equipped with a Rheodyne 7161 injector (20-μL loop). Peaks were detected at 225 nm with a Spectra Physics forward optical scanning detector. Data acquisition and integration employed Dynamax software from Rainin (Woburn, MA). A mobile phase of 10 mM sodium phosphate, pH 7.4, with variable amounts of lithium perchlorate was used at a flow rate of 0.5 mL/min.

Analytical Centrifugation. Equilibrium and velocity experiments were performed with a Beckman Optima XL-A analytical ultracentrifuge as described previously (Mach et al., 1993). Acidic FGF at a concentration of 0.05 μg/mL was loaded into cells in the presence of 0, 1.2, and 2.4 M $LiClO_4$ employing a 10 mM sodium phosphate, 0.1 mM DTT, and 0.1 mM EDTA, pH 7.2, buffer at 20 °C. Centrifugation was conducted at 30 000 and 37 000 rpm for equilibrium and at 50 000 rpm for velocity experiments. Using 15 900 Da as the molecular mass value for aFGF (Burgess & Maciag, 1989), the partial specific volume at each lithium perchlorate concentration was calculated using a least-squares fit of the log absorbance vs radius data to the sedimentation equilibrium equation (van Holde, 1975). Sedimentation coefficients were calculated from the time derivatives of the sedimentation velocity concentration profiles using methodology and software generously provided by Dr. W. F. Stafford III (Stafford, 1992).

Differential Scanning Calorimetry. Calorimetry experiments were performed with a Hart 7708 differential scanning calorimeter employing a scan rate of 60 °C/h and a 1 mg/mL protein concentration. Differences between thermograms of aFGF at pH 2.2 in the presence and absence of heparin (0.3×) and aFGF in 0.1 M $LiClO_4$ at pH 7.0 were minimal.

RESULTS

The far-UV CD spectrum of aFGF at pH 7 (10 mM sodium phosphate) is dominated by a strong negative peak at 205 nm and broad positive ellipticity centered near 225 nm (Figure 1, curve 1). Such a spectrum is characteristic of β-sheet-rich proteins of the β-II type (Wu et al., 1992). The positive peak between 220 and 240 nm presumably results, at least partially, from an aromatic contribution to the spectrum since aFGF does not contain disulfide bonds under these conditions. Lowering of the pH of aFGF solutions to 2.2 produces a dramatic increase in the magnitude of the negative ellipticity band and a 3–4-nm shift to lower wavelength, consistent with significant unfolding of the protein. In addition, the positive 225-nm peak is lost and replaced by a negative shoulder in

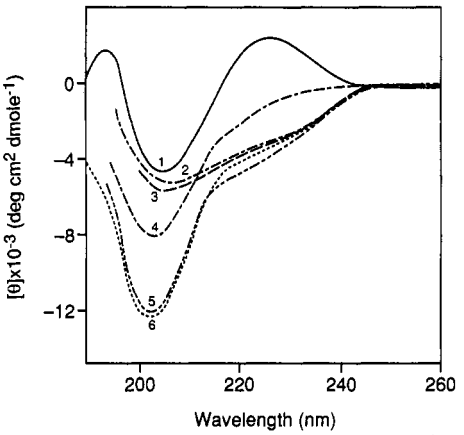

FIGURE 1: Far-UV CD spectra of aFGF under various solution conditions. Samples contained 0.1 mg/mL aFGF in 10 mM sodium phosphate, 0.1 mM EDTA, and 1 mM DTT at 20 °C. The pH was adjusted with 1 N HCl. From top to bottom: 1, pH 7 (native); 2, pH 2.2, 0.75 μM heparin; 3, pH 2.2, 0.1 M $LiClO_4$; 4, pH 7, 1.2 M $LiClO_4$; 5, pH 7, 3.6 M $LiClO_4$; 6, pH 2.2, no additions. For a description of the CD measurements, see Materials and Methods.

the same region, consistent with disruption of tertiary structure (Figure 1, curve 6). No light-scattering evidence of protein aggregation is apparent under these low-pH, low ionic strength conditions. A very similar spectrum is observed when the protein is unfolded at neutral pH by 3.6 M $LiClO_4$ (Figure 1, curve 5).

Addition of subdenaturing concentrations of chaotropic agents (e.g., 1.2 M $LiClO_4$) to aFGF at pH 7 produces a spectrum intermediate between that of native and unfolded protein with only half the decrease seen in the 205-nm band compared to the pH 2.2 spectrum but substantial loss of the 225-nm signal (Figure 1, curve 4). Fluorescence experiments, to be described later, indicate that the conversion to a species characterized by such spectra is complete at 1.0–1.2 N $LiClO_4$ (see Table I). In contrast, at pH 2.2, addition of $LiClO_4$ or heparin results in a spectrum with a 205-nm negative ellipticity band like that of native protein but loss of the 225-nm positive signal as seen in unfolded aFGF (Figure 1, curves 2 and 3). These effects are complete at 0.1 M $LiClO_4$ and 0.75 μM heparin. Similar to heparin, 6 mM Na_2SO_4 stabilizes aFGF at neutral pH (Volkin et al., 1993). Sodium sulfate concentrations like those required for other inorganic salts (>0.1 M), however, are necessary to obtain CD spectra comparable to those produced by heparin (not illustrated). After several minutes of incubation in the presence of salts, significant turbidity due to concentration-dependent protein aggregation begins to occur, and reliable spectral data cannot be obtained.

The secondary structure of aFGF was also examined by amide I′ FTIR under various solution conditions. The deconvoluted spectrum of the native protein at pD 7 is dominated by peaks associated with β-structure at 1628, 1637, and 1678 cm^{-1} as well as contributions from turns at 1662, 1669, and 1690 cm^{-1} (Figure 2) (Byler & Susi, 1986; Copeland et al., 1991). The other two major signals at 1646 and 1653 cm^{-1} presumably arise from loops and various types of nonrepetitive structure since aFGF lacks α-helical regions (Zhu et al., 1991; Middaugh et al., 1992) which usually absorb in this region. Addition of 1.2 M $LiClO_4$ at pD 7 or lowering of the solution pD to 2 in either the presence or the absence of heparin results in a spectrum in which major peaks are now found between 1605 and 1620 cm^{-1}. Such signals can be assigned to the formation of intermolecular β-structure in associated protein (Ismail et al., 1992; Jackson & Mantsch, 1992). Subtraction of this spectral contribution, however, permits the remaining portion of the spectrum to be used to probe secondary structure content. This analysis finds approximately 45% β-sheet, 20% turn, and 35% less ordered structure in the native protein (pD 7) as well as a similar secondary structure content at pD 2 in the presence of heparin. The deconvoluted amide I′ spectrum of aFGF at pD 7 in the presence of 1.2 M $LiClO_4$ suggests a slight increase in β-sheet and turn structure (50% and 25%, respectively) and an accompanying decrease (25%) in random polypeptide content compared to native growth factor. Complete unfolding of aFGF with 3.6 M $LiClO_4$ at pH 7 or by low pD in the absence of stabilizing anion results in a spectrum dominated by a peak due to disordered structure in the 1646–1650-cm^{-1} region (not illustrated).

Although aggregation does not permit near-UV CD spectra to be reliably measured at low pH, such data can be obtained at pH 7 in the presence of $LiClO_4$. The native protein at pH 7 produces a well-defined series of negative peaks between 260 and 300 nm (Figure 3). Unfolding of the protein with 3.6 M $LiClO_4$ at neutral pH causes loss of these negative bands which are replaced with positive ellipticity near 260 nm. The presence of an intermediate concentration of $LiClO_4$ (1.2 M) results in a spectrum similar to that of the unfolded protein with the new 260-nm band less pronounced.

Similar studies of the effect of low pH and anions on the intrinsic fluorescence emission spectrum of aFGF were also conducted (Figure 4). Native aFGF (pH 7, curve 6) produces primarily tyrosine fluorescence with an emission peak at ca. 304 nm. The fluorescence of the protein's single tryptophan residue is strongly quenched in its native state, but can be detected by selective excitation with incident light above 295 nm (not illustrated) (Copeland et al., 1991). When the structure of the protein is disrupted by low pH at low ionic strength or by the presence of high concentrations of a chaotropic agent (3.6 M $LiClO_4$) at neutral pH, this quenching is relieved, and tryptophan emission centered near 340 nm is apparent (Figure 4, curves 3 and 5). Selective tryptophan excitation produces an emission band centered at approximately 348 nm, consistent with complete solvent exposure (not shown). Addition of moderate concentrations of $LiClO_4$ (1.2 M) at pH 7 induces emission spectra similar to those of the unfolded forms (Figure 4, curve 4). In contrast, addition of 0.1 N $LiClO_4$ or 0.75 μM heparin at pH 2 causes a much greater increase in the fluorescence emission of the indole moiety with a 6–8-nm decrease in the wavelength position of the emission peak (Figure 4, curves 1 and 2). This increase in emission is sufficiently large that the tyrosine peak is more obscured than seen in other situations.

The above observations suggest that aFGF may be transformed into an MG state in the presence of anions at low pH and at intermediate chaotrope concentrations under neutral conditions. Another property characteristic of MG states is their ability to bind apolar dyes such as ANS (Semisotnov et al., 1987; Ptitsyn et al., 1990). The dye itself fluoresces only weakly in solution with a broad emission maximum near 560 nm. Addition of aFGF to dye solutions at pH 7 in the presence or absence of 3.6 M $LiClO_4$ has no effect on ANS fluorescence (Table I). In contrast, a small increase in the quantum yield and a 40-nm blue shift in ANS fluorescence are observed in the presence of aFGF at pH 2.2 and low ionic strength. When anions (0.1 M $LiClO_4$, 0.75 μM heparin) are added to a pH 2.2 aFGF solution, a much greater increase in intensity and a blue shift of ANS fluorescence are apparent (Table I), indicating binding of the dye under these conditions. A similar result is seen at neutral pH in the presence of 1.2 M $LiClO_4$.

Table I: ANS Binding and Urea Denaturation Parameters for aFGF under Various Solution Conditions[a]

conditions	ANS binding		urea unfolding		
	rel fluorescence intensity at 480 nm	λ_{max} (nm)	$\Delta G°_{unf}$ (kcal·mol^{-1})	$[urea]_{1/2}$ (M)	*m* cooperativity parameter (kcal·mol^{-1}·M^{-1})
no aFGF	0.5	560			
pH 2.2	2	490			
pH 2.2, 0.75 μM heparin	7	480		>6	
pH 2.2, 0.1 M $LiClO_4$	30	480	4.5 ± 0.4[b]	1.8 ± 0.3	2.4 ± 0.3
pH 7	0.5	560	6.5 ± 0.3	2.3 ± 0.2	2.9 ± 0.2
pH 7, 1.2 N $LiClO_4$	8	475	2.3 ± 0.4[b]	2.0 ± 0.2	1.1 ± 0.2

[a] The various postulated molten globule states (conditions) were prepared as described under Materials and Methods. Fluorescence emission spectra of ANS were collected between 400 and 600 nm with excitation at 320 nm. The wavelength of maximum fluorescence (λ_{max}) was determined as the position of the intersection of the first-derivative emission spectrum with the wavelength axis. The following thermodynamic relations were employed to analyze the unfolding transitions (Pace, 1975; Cupo & Pace, 1983): $\Delta G_{unf} = -RT \ln([N]/[U])$ and $\Delta G_{unf} = \Delta G°_{unf} - m[D]$, where ΔG_{unf} and $\Delta G°_{unf}$ are Gibb's free energies of unfolding in the presence and absence of chaotrope, respectively. [N], [U], and [D] are the concentrations of native or MG aFGF, unfolded aFGF, and denaturing agent, respectively, and *m* is a parameter reflecting the cooperativity of unfolding. [b] Due to deviations from two-state behavior, these values of $\Delta G°_{unf}$ are apparent only. 95% confidence limits are shown.

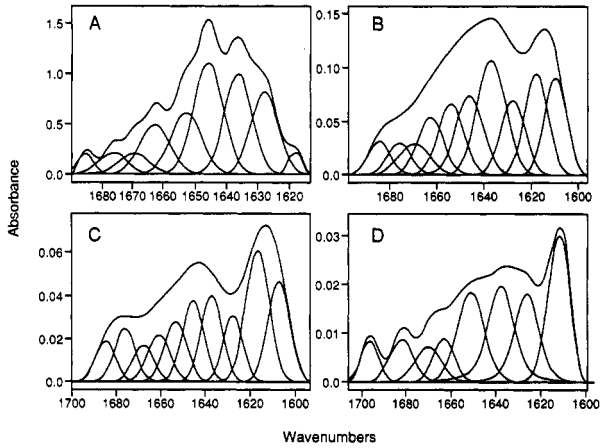

FIGURE 2: Deconvoluted amide I′ FTIR spectra of aFGF under various solution conditions. (A) pD 7 (native); (B) pD 2, 4 μM heparin; (C) pD 2, 0.1 M $LiClO_4$; (D) pD 7, 1.2 M $LiClO_4$. All spectra were obtained in D_2O at a protein concentration of 0.5 mg/mL. See the text for a discussion of the deconvolution procedure.

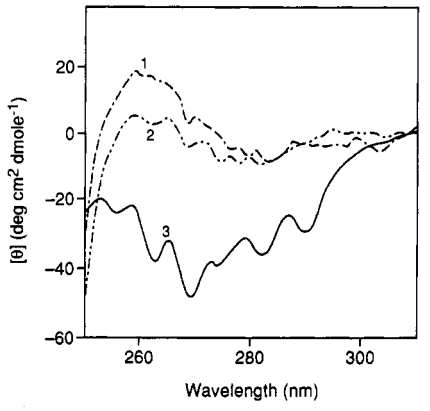

FIGURE 3: Representative near-UV CD spectra of aFGF. 1, pH 7, 3.6 M $LiClO_4$ (unfolded); 2, pH 7, 1.2 M $LiClO_4$; 3, pH 7 (native). Spectra are corrected for the background CD signal of a 10 mM sodium phosphate buffer. A protein concentration of 1 mg/mL (1-cm path length) at 20 °C was employed.

One useful method of comparing protein stability is the measurement of the amount of structure present as a function of denaturing agent concentration. Urea was found suitable for unfolding of the various postulated MG states. Since the stability of these states is dependent on ionic interactions, the use of a nonionic perturbant such as urea simplifies interpretation of unfolding phenomena. At neutral pH, a well-defined cooperative unfolding transition centered at 2.3 M urea was observed for native aFGF (Mach et al., 1992; Burke et al., 1993) which yielded a value for the free energy of unfolding extrapolated to zero urea concentration ($\Delta G°_{unf}$) of 6.5 ± 0.3 kcal/mol (Table I). The slope of the $-RT$ ln ([N]/[U]) versus urea concentration plot used to estimate the value of $\Delta G°_{unf}$ was equal to 2.9, reflecting the highly cooperative nature of the unfolding process. In the case of both the acidic and neutral $LiClO_4$-induced MG states, the values of this cooperativity parameter were significantly less, and the transition midpoints occurred at approximately 20% lower urea concentrations. These latter thermodynamic analyses also yielded apparent values of $\Delta G°_{unf}$, but the low values of the cooperativity parameters suggest that the free energy values cannot be meaningfully interpreted. In contrast to the salt-induced conformational state at low pH, the presence of heparin at low pH induced a species that was resistant to urea disruption at concentrations greater than 6 M. Attempts were also made to examine the unfolding of the MG state by differential scanning calorimetry. As observed by others (Yutani et al., 1992), only very weak, poorly reproducible endothermic transitions were seen. At the protein concentrations necessary for these experiments (>0.5 mg/mL), however, a large exothermic peak was observed coincident with protein aggregation.

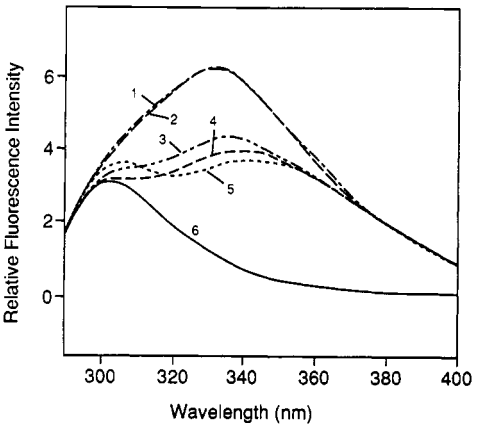

FIGURE 4: Intrinsic aromatic amino acid fluorescence emission spectra of aFGF under various solution conditions. Solution conditions identical to those used in far-UV CD spectroscopy were employed (Figure 1). Spectra were collected between 290 and 400 nm with excitation at 270 nm at 20 °C. From top to bottom: 1, pH 2.2, 0.75 μM heparin; 2, pH 2.2, 0.1 M $LiClO_4$; 3, pH 7, 3.6 M $LiClO_4$; 4, pH 7, 1.2 M $LiClO_4$; 5, pH 2.2, no additions; 6, pH 7 (native). The apparent fluorescence intensity of aFGF at pH 2.2 in the presence of anions deteriorated with time due to aggregation-induced effects. Spectra obtained prior to detectable aggregation are shown.

To further explore the effect of pH itself (i.e., high chloride anion concentration) on the structure of aFGF, far-UV CD,

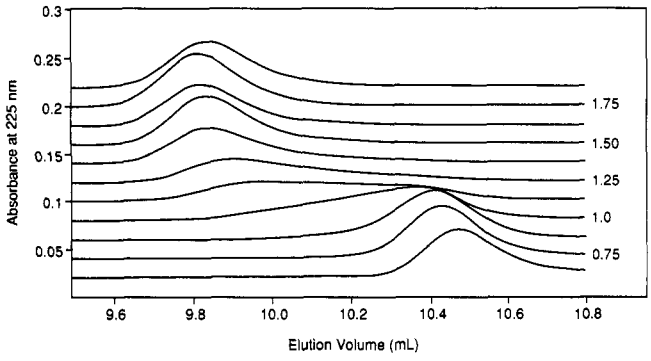

FIGURE 5: Size-exclusion chromatography of aFGF in $LiClO_4$ solutions. Twenty microliters of 0.05 mg/mL aFGF in 10 mM sodium phosphate, pH 7.2, and variable concentrations of $LiClO_4$ were injected onto a 0.78 × 30 cm HPLC SEC column preequilibrated at the same $LiClO_4$ concentrations and eluted at a flow rate of 0.5 mL/min. The bottom elution profile was obtained at 0.5 M $LiClO_4$, and the top one at 2.0 M $LiClO_4$. Profiles from intermediate $LiClO_4$ concentrations are as indicated. See Materials and Methods for more details.

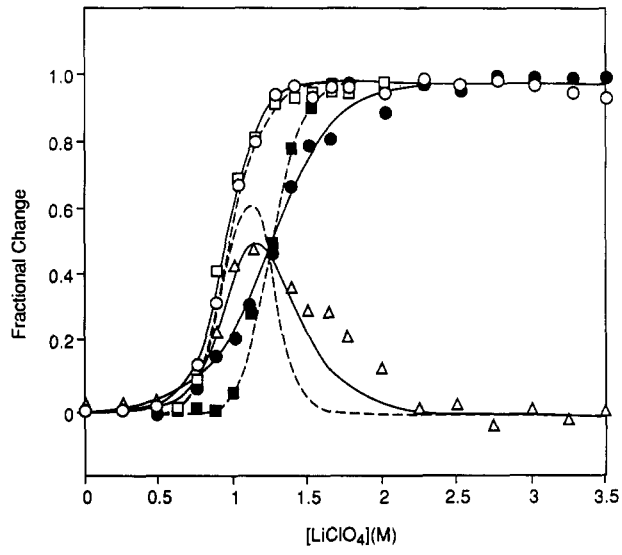

FIGURE 6: Fractional changes of relevant spectroscopic and hydrodynamic properties during unfolding of aFGF in lithium perchlorate. The loss of tertiary structure was detected by the fluorescence emission at 340 nm (○) and the absorbance at 225 nm at an SEC elution volume of 10.4–10.5 mL (□) (Figure 5). The appearance of the fully unfolded state was detected by the CD signal at 205 nm (●) and the absorbance at 225 nm at an elution volume of 9.83 mL (■). The solid and dashed lines are obtained by a nonlinear least-squares fit assuming a two-state model of the transitions (Pace, 1975) from the spectroscopic and hydrodynamic data, respectively. The Gaussian-shaped peaks are the difference between the corresponding tertiary/secondary structural transitions. The intensity of ANS fluorescence at 480 nm (△) was normalized to permit comparison of the peaks. Spectroscopic data were corrected for base-line shifts by least-squares fitting of straight lines outside the transition regions and dividing the difference between the data point and lower line by the vertical distance between these lines.

intrinsic fluorescence, and optical density (280 nm) measurements were performed from apparent pH 6 to 0. Below pH 1.0, where the ionic strength reaches the level which normally induces partially structured conformations at pH 2.2, the ratio of the CD signals at 205 nm to 225 nm decreased, and the fluorescence 340/300-nm ratio increased, indicating the formation of similar states. The overall decrease of spectroscopic signal intensities and subsequent onset of turbidity indicated aggregation of these species (not illustrated).

Size-exclusion chromatography was used to investigate the hydrodynamic dimensions of these partially folded states (Figure 5). In its native form, aFGF elutes at an elution volume of approximately 10.5 mL employing a Toso-Haas G3000 SW_{XL} column. Elution time was found to be dependent on ionic strength because significant interaction of aFGF with the column matrix occurs at $LiClO_4$ concentrations below 0.5 M. At least 0.2 M NaCl is required to assure similar elution volumes in the absence of $LiClO_4$ (not shown). The appearance of more rapidly eluting, less compact species at $LiClO_4$ concentrations between 1.0 and 1.25 M coincides with the concentration range at which transitions are observed by spectroscopic methods. Further increases in $LiClO_4$ concentration yield elution volumes of approximately 9.8 mL, corresponding to unfolded aFGF as detected by CD, FTIR, and fluorescence spectroscopy (Figures 1–4).

Interestingly, the marked chromatographically detected changes in the hydrodynamic properties of aFGF induced by lithium perchlorate were not resolved by analytical ultracentrifugation. No change in the partial specific volume of aFGF was detected between native and unfolded states as judged by sedimentation equilibrium profiles at 30 000 and 37 000 rpm (not shown). Sedimentation coefficients obtained from velocity studies at 50 000 rpm were 2.03 S in aqueous buffer, 1.51 S in 1.2 M $LiClO_4$, and 1.15 S in 2.4 M $LiClO_4$. These differences, however, were entirely accounted for by differences in $LiClO_4$-dependent solvent densities, and consequently, the corrected values differed by less than 2% (not illustrated). One possible explanation for this finding is that lithium perchlorate molecules are being preferentially bound by unfolded and partially folded polypeptide, resulting in densities higher than those expected for acid-denatured proteins (Buchner et al., 1991).

The ability of $LiClO_4$ both to induce a molten globule state at pH 7 and, at sufficiently high concentrations, to unfold aFGF is summarized in Figure 6 in terms of the fractional change of the relevant spectroscopic and hydrodynamic parameters. As expected, the disappearance of the native SEC peak coincides with the appearance of tryptophan fluorescence which indicates disruption of tertiary structure. Completely unfolded species as detected by CD and SEC appear at chaotrope concentrations about 0.4 M higher. The appearance of the chromatography peak corresponding to the unfolded form, however, appears to be more cooperative than the loss of secondary structure as judged by CD. The fractional content of the partially folded species predicted from the relative content of the native and unfolded forms falls in the region of increased ANS binding (Figure 6).

The studies described above suggest that aFGF can form distinct MG-like states under equilibrium conditions at low pH and high anion concentration as well as at neutral pH in the presence of moderate concentrations of a chaotropic agent. Part of the intense interest in such conformational forms, however, arises from the possibility that similar states occur early in the folding pathway of proteins. We therefore searched for evidence that these forms might be present in the refolding pathway of aFGF. Figure 7 illustrates the time-dependent fluorescence spectra of aFGF and ANS as solutions containing both entities are diluted from 2 to 0.2 M guanidine hydrochloride, a procedure in which the protein efficiently refolds over a period of minutes (Dabora et al., 1991). As previously shown, the tryptophan emission is quenched as the protein regains its native state (Copeland et al., 1991). In addition, the ANS peak above 500 nm is also quenched and shifted to longer wavelength, indicating a concomitant decrease in binding of the hydrophobic probe as aFGF refolds. Similar experiments were conducted by diluting unfolded aFGF in

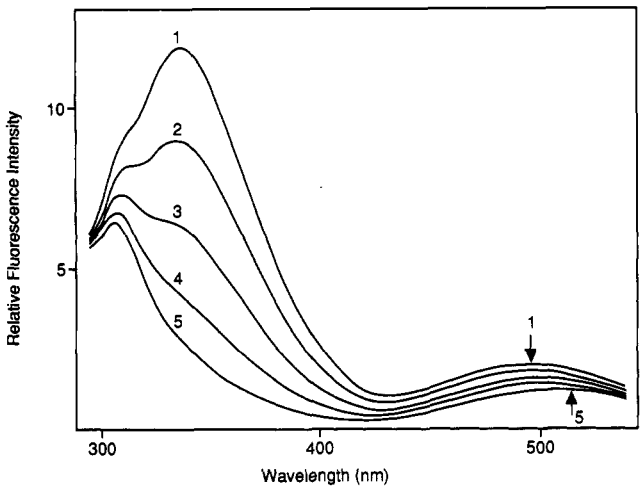

FIGURE 7: Kinetics of the refolding of aFGF at pH 7 as monitored by fluorescence spectroscopy. An aFGF (0.5 mg/mL) solution containing 2 M guanidine hydrochloride and 0.5 mM ANS was diluted 10-fold into buffer, and fluorescence spectra (excitation at 270 nm) between 290 and 550 nm were collected every minute. Spectra are shown at (1) 1, (2) 2, (3) 4, (4) 8, and (5) 16 min. A 10 mM sodium phosphate, 0.1 mM EDTA, and 1 mM DTT, pH 7, buffer was used at 15 °C. The ANS emission peak positions at 1 and 16 min (after complete refolding) are indicated with arrows.

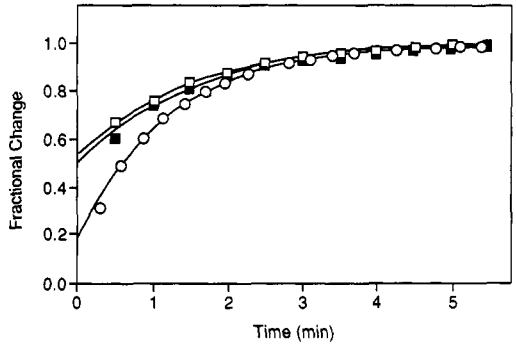

FIGURE 8: Kinetics of refolding of aFGF at pH 7 as probed by both CD and fluorescence. An aFGF (0.5 mg/mL) solution containing 3.6 M $LiClO_4$ was diluted 6-fold, and CD spectra were measured every 30 s. The initial CD values at 205 and 230 nm, extrapolated to zero time, coincide with the corresponding values for aFGF in 1.2 N $LiClO_4$. CD values at 230 nm (□) and at 205 nm (■) are shown. The intrinsic Trp fluorescence was also used to monitor refolding (○). The solid lines represent a least-squares fit to a first-order rate equation. Experiments were performed in sodium phosphate buffer at 15 °C.

3.6 M $LiClO_4$ at pH 7 6-fold and then monitoring refolding by both CD and intrinsic protein fluorescence. It is apparent in the first minute of the refolding process that the structural features monitored by CD both at 205 nm and, in part, at 225 nm are more rapidly gained than those reflected by the more tertiary structure sensitive indole fluorescence emission (Figure 8). In fact, some portion of the 205- and 225-nm CD signal changes is probably due to changes in the optical activity of aromatic amino acids, thus also reflecting the tertiary structure transitions detected by the intrinsic Trp fluorescence. Attempts to follow the creation of secondary structure at earlier times by stopped-flow CD at these wavelengths found that the majority of the spectroscopic change was complete within the dead-time of the instrument (10 ms; results not illustrated).

To investigate earlier events in the refolding process, stopped-flow experiments were performed employing ANS as a probe of the protein's conformational state. When the pH of an aFGF solution containing ANS is jumped from 2.2 to 7, there is an initial rapid increase in ANS fluorescence (Figure 9) which after 200 ms begins to decay with first-order kinetics

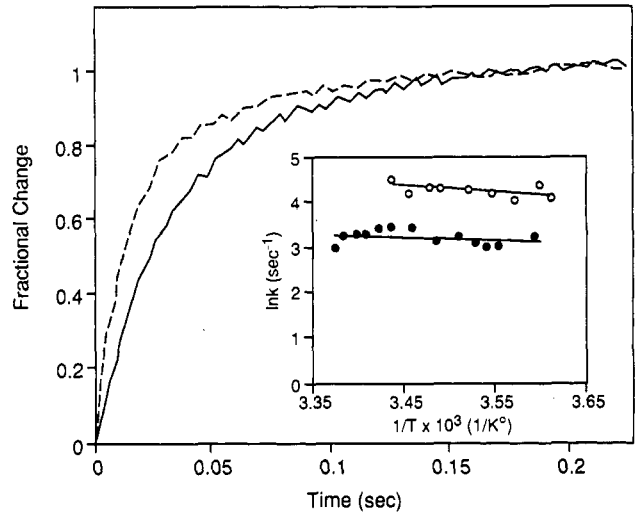

FIGURE 9: Stopped-flow kinetics of refolding of aFGF (0.1 mg/mL) at pH 7 monitoring ANS fluorescence (excitation 320 nm, emission >350 nm). Refolding of aFGF from a pH 2.2 10 mM sodium phosphate solution was induced by 1:1 mixing with 50 mM sodium phosphate, pH 7.5 (solid line), and refolding from 2.0 M $LiClO_4$/10 mM sodium phosphate, pH 7, produced by 1:1 mixing with 10 mM sodium phosphate, pH 7 (dashed line). The concentration of ANS was 150 μM. Inset: Arrhenius plot of MG state formation during the pH jump (○) and from a $LiClO_4$ dilution from 2 M to 1 M (●). The lines are drawn from a least-squares fit of the data to the Arrhenius equation. Buffer containing 10 mM phosphate supplemented with 0.1 mM EDTA and 1 mM DTT was employed.

($t_{1/2}$ ~7 s) (not illustrated). If an aFGF/ANS solution at pH 7 in 2.0 M $LiClO_4$ is rapidly diluted to 1.0 M salt, partial refolding of the protein is induced (i.e., a mixture of the native and MG states). There is a similar increase in fluorescence over the initial 200 ms (Figure 9), but only limited decay occurs. We have examined the temperature dependence of the kinetics of the initial major (~80%) phase of the partially structured intermediate formation, and found only a weak effect between 3 and 23 °C (inset, Figure 9). The activation energies were found to be 2.7 ± 3.0 and 1.5 ± 2.3 kcal/mol for the lithium perchlorate and low-pH/salt-induced MG states, respectively. This compares to an approximately 14 kcal/mol activation energy for the subsequent tertiary structure forming, slow-refolding step (Dabora et al., 1991).

DISCUSSION

It is apparent from this work that it is possible to induce what are now conventionally referred to as molten globule states in aFGF. For example, when the pH of aFGF solutions is lowered beyond the ionization point of carboxylic residues and moderate to high concentrations of an anionic species are present (e.g., 0.1 M HCl, 0.1 M $LiClO_4$, 0.1 μM heparin), both far-UV circular dichroism and amide I′ FTIR clearly indicate the presence of a protein with secondary structure content similar to that of the native state. It is less clear whether the same sequence-related elements of secondary structure are present in both native and MG forms, but the similarity in the CD and FTIR spectra of all species examined would suggest that this is quite possible. Unlike most proteins so far examined [for exceptions, see Jiskoot et al. (1991) and Bychkova et al. (1992)] which are primarily α-helical in nature, aFGF is a pure β-sheet-containing protein (Zhu et al., 1991). Thus, such proteins are also readily capable of forming MG states. A similar form of the protein can also be induced by moderate concentrations of chaotropic agents at neutral pH. Lithium perchlorate was chosen for these studies because of its optical transparency in the far-UV region and its strong

chaotropic properties (Denton et al., 1982; Lynn et al., 1984). However, other chaotropic salts and agents such as guanidine hydrochloride are also able to induce MG states in aFGF (not illustrated). In addition, we have previously observed that when the thermal unfolding of aFGF is monitored by both intrinsic tryptophan fluorescence and far-UV CD, the melting temperature (T_m) obtained from the former measurements is approximately 7 °C lower (Copeland et al., 1991). This apparent disruption of the protein's tertiary structure prior to loss of its β-sheet elements suggests that aFGF also forms a thermally induced MG state between these two events. Interestingly, the temperature range over which this occurs (30–40 °C) is of physiological relevance. Recent reports that passive membrane translocation of aFGF may require structurally disrupted protein (Wiedlocha et al., 1992) and that heat shock can cause the release of aFGF from cells (Jackson et al., 1992) suggest that the temperature-induced MG state of aFGF could be of some functional utility (Bychkova et al., 1988).

Consistent with previously described properties of the MG state, low pH and high anion concentration as well as chaotropes at neutral pH induce a form of the protein that appears to be low in overall tertiary structure despite the presence of extensive β-sheet. This is evident in near-UV CD spectra where transitions due to tertiary structure induced optical activity in aromatic groups are abolished under MG conditions. Some tertiary structure does appear to be present, however, although it is much reduced compared to the native state. In the intrinsic fluorescence emission spectrum of native aFGF, the tertiary structure induced presence of a histidine residue near the protein's single indole appears to cause this moiety to be quenched (Copeland et al., 1991; Zhu et al., 1991). Thermal unfolding of the protein abolishes this quenching, resulting in significant fluorescence emission near 340 nm (Copeland et al., 1991). In contrast, the MG states of aFGF manifest an indole emission peak shifted to lower wavelength (e.g., ca. 330 nm) and with a significantly enhanced intensity relative to more extensively unfolded states. This suggests that the Trp residue of aFGF in MG states is in a more apolar environment than in extensively disordered forms of the protein. The precise environment of the Trp residue in such forms of the protein remains to be defined, however, and no direct evidence for the retention of any nativelike tertiary structure can be ascertained from these observations.

The nature of the MG state can be further probed by the binding of apolar dyes such as ANS since unlike native and unfolded conformations of proteins, this form appears to generally bind such hydrophobic chromophores with a subsequent enhancement in dye fluorescence (Semisotnov et al., 1987; Ptitsyn et al., 1990). Direct perturbation of protein structure by ANS itself appears to be minimal, since the time-dependent intrinsic Trp fluorescence spectra of aFGF during refolding were identical in the presence and absence of ANS (not illustrated). It is noteworthy that far-UV CD spectra of acid-denatured (pH 2.2, low ionic strength) and lithium perchlorate-denatured aFGF are essentially identical, while ANS fluorescence is enhanced in the acidic state. This may simply reflect the decreased charge density of the protein as a consequence of protonation of carboxylic groups which in turn might enhance ANS binding independently of the protein's conformational state. As shown in Table I, there is a surprising degree of variability of induced ANS fluorescence in the presence of aFGF with 0.1 M $LiClO_4$, pH 2.2 > 1.2 M $LiClO_4$, pH 7 > 0.75 μM heparin, pH 2.2 > pH 2.2 > pH 7. It is thus apparent that the various MG forms differ significantly in their ability to enhance ANS fluorescence, presumably reflecting subtle differences in their degree of tertiary structure. This could arise from differences in the accessibility of MG apolar surfaces to the dye, the existence of specific binding sites unique to each form, and/or variability in the overall polarity and degree of aggregation of the MG states. Similar to numerous other proteins exhibiting concentration-dependent aggregation of partially folded states, aFGF manifested slow, time-dependent aggregation upon assumption of any of the various partially structured states. Lithium perchlorate-induced MG states retained the best solubility and thus were more thoroughly characterized. Measurement of physical parameters obtained before significant aggregation, however, revealed typical MG properties for these species. In contrast, fully denatured states exhibited good solubility. These observations suggest that at least in the case of aFGF, the fully unfolded protein is not responsible for the precipitation observed under a wide variety of environmental conditions. Rather it is the MG forms that account for the presence of aggregated material. It seems possible that this conclusion may be more widely applicable. For example, aggregation of partially or improperly folded polypeptide chains is believed to play a role in Alzheimer's disease (Spencer et al., 1991; Tomski & Murphy, 1992) and related disorders (Glenner, 1980a,b). Similar aggregation phenomena may occur in inclusion bodies formed from protein overexpressed in host cells (Mitrabi & King, 1989; Bowden et al., 1991) and in the formation of cataracts (Harding & Crabbe, 1984). Interestingly, recent reports (Horwitz, 1992; Jakob et al., 1993; Merck et al., 1993) demonstrate that major lens proteins may act as molecular chaperones.

Another distinguishing characteristic of the MG state is its compactness, which is thought to be intermediate between that of native and unfolded conformations (Creighton & Pain, 1980; Goto & Fink, 1989; Ptitsyn et al., 1990; Chaffotte et al., 1991; Jang & Englander, 1991; Zerovnik et al., 1992; Bychkova et al., 1992). Size-exclusion elution profiles (Figure 5) reveal the presence of such globular species under conditions of MG formation (e.g., enhanced ANS binding) where the tertiary structure appears to be lost and the secondary structure remains largely intact (Figures 1–6). Although the appearance of species at intermediate elution volumes can also be consistent with two-state behavior if equilibrium at a given denaturant concentration has not been reached at the time of chromatography (Endo et al., 1983; Shalongo et al., 1987), the markedly shifted peaks of presumably structurally altered aFGF in 1.125 and 1.25 M $LiClO_4$ (Figure 5, 9.9–10.0 elution volumes) argue that distinct intermediates must be present. In order to assess the thermodynamics of these states, we induced unfolding of the MG states employing $LiClO_4$ and urea as structural perturbants. These studies (Figures 7–9) demonstrate the existence of protein forms at low pH and high anion concentration or at neutral pH in the presence of moderate amounts of a chaotropic agent with extensive secondary but low tertiary structure content that gradually (noncooperatively) lose these physical properties upon addition of urea and other structure-disrupting solutes. These transitions display only weak endotherms in DSC experiments as reported by Yutani et al. (1992), suggesting a primarily entropic origin. Nevertheless, these presumptive MG states are remarkably stable in certain cases (Table I). For example, although the MG state induced by 0.1 M $LiClO_4$ at pH 2.2 was disrupted by 1–3 M urea, the 0.75 μM heparin-induced form at pH 2.2 was stable at urea concentrations exceeding 6 M. This raises the question as to whether heparin might

be binding to specific sites on the MG aFGF molecule as it does to the native form. In fact, the binding site on native aFGF for heparin and other anions is relatively nonspecific (Volkin et al., 1993). It is therefore possible that an MG binding site for anions exists that may or may not be similar to that of the native state. The apparent lack of strict tertiary structure requirements for such a site is supported by the observation that a number of growth factor peptides are capable of strongly interacting with heparin (Baird et al., 1988; Mehlman & Burgess, 1990). These observations may be of some biological relevance since aFGF can be found in acidic environments where it might be stabilized in the MG state by some specific polyanion. The biological activity, or lack thereof, of any MG form of the protein remains to be ascertained. Alternatively, the very high ionic strength of a 0.75 μM heparin solution is comparable to that of salt-induced MG states. Thus, the charge neutralization of the protein at low pH that is thought to be primarily responsible for the collapse into the MG state (Dill, 1990) may still be the primary effect seen with lower concentrations of the heavily sulfated polysaccharides. We are currently testing the possibility that specific binding sites for polyanions might still exist in the MG states of aFGF.

The potential relationship of these equilibrium MG states to any early folding intermediates is of significant interest. Previous studies of the kinetics of refolding of aFGF suggested the existence of a rapidly formed intermediate that is not significantly affected by the presence of polyanions (Dabora et al., 1991). Indeed, a striking similarity does seem to exist between the MG equilibrium forms identified in this study and the structure of aFGF early in its folding pathway. Simultaneous circular dichroism and fluorescence measurements indicate that most of the secondary structure of the protein is formed prior to its tertiary structure. Using enhanced ANS fluorescence to detect the presence of MG states, it appears that these forms of aFGF are formed in less than a second and then gradually dissipate many seconds later. This earlier event (formation of MG) appears to involve at least two processes, with the initial phase possibly corresponding to the hydrophobic collapse that is thought to constitute MG formation. As discussed by others (Baldwin, 1991), the presence of these early spontaneous folding events of local secondary structure formation and hydrophobic collapse essentially resolves Levinthal's paradox (Dill et al., 1993; Levinthal, 1969; Zwanzig et al., 1992). An alternative to the MG concept argues that the observed data can be accounted for by the existence of the majority of the protein in its native structure with termini or loops present in a more disordered state. Careful analysis of the near-UV CD spectra of aFGF, however, reveals that most of the tertiary structure induced optical activity in all of the aromatic amino acids, viz., Trp ($\sim$290 nm), Tyr (270–280 nm), and Phe (255–265 nm), is lost in the MG state. Examination of the crystal structure of the FGFs finds that most Tyr side chains are solvent-exposed in the native state while all six Phe and the Trp residue are at least partially buried in the protein's core (Zhu et al., 1991). Furthermore, during refolding the kinetics detected by both the Trp residue (local) and ANS (global) fluorescence are identical (see Figure 7). This strongly suggests that the formation of the MG state is a global rather than local phenomenon. Similar pH-induced kinetics of refolding of synthetic polymers support the nonspecific nature of this initial collapse (Bednar et al., 1985).

In summary, the picture that emerges from these studies is similar to that seen by others with small proteins [for example, see the discussion in Chen et al. (1992)]. Acidic FGF appears to rapidly fold into a state with β-sheet content similar to that of the native molecule. This form of the protein, however, lacks extensive tertiary contacts although evidence for some limited three-dimensional structure is evident. This early MG intermediate is presumably due to a combination of hydrophobic collapse and local secondary structure formation as postulated for other proteins, although the relationship between these two events is still ill-defined. The formation of such partially folded intermediates also correlates with irreversible aggregation. The ability to induce this state at low pH with polyanions that also stabilize the native form of the protein under neutral conditions is provocative, but the biological significance of this observation, if any, remains to be better defined. Nevertheless, the potential existence of MG forms of aFGF under physiological conditions and the potential transport competence of these states (Bychkova et al., 1988; Wiedlocha et al., 1992) are consistent with their biological relevance.

ACKNOWLEDGMENT

We thank Dr. William Randall for help with the stopped-flow fluorescence studies, Mr. Jeff Campbell for graphic support, Dr. G. Sanyal for helpful discussion, and Dr. John Ryley of Applied Photophysics for the stopped-flow CD measurements. We also thank Drs. S. Yamazaki, R. Sitrin, and C. Orella for supplying the large amounts of purified aFGF employed in these studies, and Laurie Rittle for manuscript preparation.

REFERENCES

Baird, A., Schubert, D., Ling, N., & Guillemin, R. (1988) *Proc. Natl. Acad. Sci. U.S.A. 85*, 2324–2328.

Baldwin, R. L. (1991) *Chemtracts: Biochem. Mol. Biol. 2*, 379–389.

Bednar, B., Morawetz, H., & Shafer, J. A. (1985) *Macromolecules 18*, 1940–1944.

Bowden, G. A., Paredes, A. M., & Georgian, G. (1991) *Bio/Technology 8*, 725–737.

Buchner, J., Renner, M., Lilie, H., Hinz, H.-J., & Jaenicke, R. (1991) *Biochemistry 30*, 6922–6929.

Burgess, W. H., & Maciag, T. (1989) *Annu. Rev. Biochem. 58*, 575–606.

Burke, C. J., Volkin, D. B., Mach, H. & Middaugh, C. R. (1993) *Biochemistry* (in press)

Bychkova, V. E., Pain, R. H., & Ptitsyn, O. B. (1988) *FEBS Lett. 238*, 231–234.

Bychkova, V. E., Berni, R., Rossi, G. L., Kutyshenko, V. P., & Ptitsyn, O. B. (1992) *Biochemistry 31*, 7566–7571.

Byler, D. M., & Susi, H. (1986) *Biopolymers 25*, 469–487.

Chaffotte, A., Guillou, Y., Delepierre, M., Hinz, H.-J., & Goldberg, M. E. (1991) *Biochemistry 30*, 8067–8074.

Chen, B.-L., Baase, W. A., Nicholson, H., & Schellman, J. A. (1992) *Biochemistry 31*, 1464–1476.

Christensen, H., & Pain, R. H. (1991) *Eur. Biophys. J. 19*, 221–229.

Copeland, R. A., Ji, H., Halfpenny, A. J., Williams, R. W., Thompson, K. C., Herber, W. K., Thomas, K. A., Bruner, M. W., Ryan, J. A., Marquis-Omer, D., Sanyal, G., Sitrin, R. D., Yamazaki, S., & Middaugh, C. R. (1991) *Arch. Biochem. Biophys. 289*, 53–61.

Creighton, T. E., & Pain, R. H. (1980) *J. Mol. Biol. 137*, 431–436.

Cupo, J. F., & Pace, C. N. (1983) *Biochemistry 22*, 2654–2658.

Dabora, J. M., Sanyal, G., & Middaugh, C. R. (1991) *J. Biol. Chem. 266*, 23637–23640.

Denton, J. B., Konishi, Y., & Sheraga, H. A. (1982) *Biochemistry 21*, 5155–5163.

Dill, K. A. (1990) *Biochemistry 29*, 7133–7155.
Dill, K. A., Fiebig, K. M., & Chan, H. C. (1993) *Proc. Natl. Acad. Sci. U.S.A. 90*, 1942–1946.
Dobson, C. M. (1992) *Curr. Opin. Struct. Biol. 2*, 6–12.
Endo, S., Saito, Y., & Wada, A. (1983) *Anal. Biochem. 131*, 108–120.
Glenner, G. G. (1980a) *N. Engl. J. Med. 302*, 1283–1292.
Glenner, G. G. (1980b) *N. Engl. J. Med. 302*, 1333–1343.
Gospodarowicz, D., & Cheng, J. (1986) *J. Cell. Physiol. 128*, 475–484.
Goto, Y., & Fink, A. L. (1989) *Biochemistry 28*, 945–952.
Harding, J. J., & Crabbe, M. J. C. (1984) in *The Eye* (Davson, H., Ed.) pp 207–492, Academic Press, Orlando, FL.
Horwitz, J. (1992) *Proc. Natl. Acad. Sci. U.S.A. 89*, 10449–10453.
Ismail, A. A., Mantsch, H. H., & Wong, P. T. T. (1992) *Biochim. Biophys. Acta 1121*, 183–188.
Jackson, A., Friedman, S., Zhan, X., Engleka, K. A., Forough, R., & Maciag, T. (1992) *Proc. Natl. Acad. Sci. U.S.A. 89*, 10691–10695.
Jackson, M., & Mantsch, H. H. (1992) *Biochem. Biophys. Acta 1118*, 139–143.
Jakob, U., Gaestel, M., Engel, K., & Buchner, J. (1993) *J. Biol. Chem. 268*, 1517–1520.
Jeng, M.-F., & Englander, S. W. (1991) *J. Mol. Biol. 221*, 1045–1061.
Jiscoot, W., Bloemendal, M., van Haeringen, B., van Grondell, R., & Beuvery, E. C. (1991) *Eur. J. Biochem. 201*, 223–232.
Kauppinen, J. K., Moffatt, D. J., Mantsch, H. H., & Cameron, D. G. (1981) *Appl. Spectrosc. 35*, 271–276.
Kuwajima, K. (1989) *Proteins: Struct., Funct., Genet. 6*, 87–103.
Levinthal, C. (1969) in *Mossbauer Spectroscopy in Biologic Systems*, Proceedings of a Meeting held at Allerton House, Monticello, IL (Debrunner, P., Tsibris, J. C. M., & Münch, E., Eds.), pp 22–24, University of Illinois Press, Urbana, IL.
Linemeyer, D. L., Kelly, L. J., Menke, J. G., Gimenez-Gallego, G., DeSalvo, J., & Thomas, K. A. (1987) *Bio/Technology 5*, 960–965.
Lynn, R. M., Konishi, T., & Sheraga, H. A. (1984) *Biochemistry 23*, 2470–2477.
Mach, H., Burke, C. J., Volkin, D. B., Dabora, J. M., Sanyal, G., & Middaugh, C. R. (1992) in *Harnessing Biotechnology for the 21st Century* (Ladisch, M. R., & Bose, A., Eds.) pp 290–293, American Chemical Society, Washington, DC.
Mach, H., Volkin, D. B., Burke, C. J., Middaugh, C. R., Linhardt, R. J., Fromm, J. R., Loganathan, D., & Mattsson, L. (1993) *Biochemistry 32*, 5480–5489.
Mehlman, T., & Burgess, W. H. (1990) *Anal. Biochem. 188*, 159–163.
Merck, K. B., Groenen, P. J. T. A., Voorter, C. E. M., de Heard-Hoekman, W. A., Horwitz, J., Bloemendal, H., & de Jong, W. W. (1993) *J. Biol. Chem. 268*, 1046–1052.
Middaugh, C. R., Mach, H., Burke, C. J., Volkin, D. B., Dabora, J. M., Tsai, P. K., Bruner, M. W., Ryan, J. A., & Marfia, K. E. (1992) *Biochemistry 31*, 9016–9024.
Mitraki, A., & King, J. (1989) *Bio/Technology 7*, 690–697.
Pace, C. N. (1975) *CRC Crit. Rev. Biochem. 3*, 1–43.
Ptitsyn, O. B., Pain, R. H., Semisotnov, G. V., Zerovnik, E., & Razgulyaev, D. I. (1990) *FEBS Lett. 262*, 20–24.
Savitzky, A., & Golay, J. E. (1964) *Anal. Chem. 36*, 1627–1639.
Semisotnov, G. V., Rodionova, N. A., Kutyshenko, V. P., Ebert, B.; Blanck, J., & Ptitsyn, O. B. (1987) *FEBS Lett. 224*, 9–13.
Shalongo, W., Ledger, R., Jagannadham, M. V., & Stellwagen, E. (1987) *Biochemistry 26*, 3135–3141.
Spencer, R. G. S., Halverson, K. J., Auger, M., McDermott, A. E., Griffin, R. G., & Lansbury, P. T., Jr. (1991) *Biochemistry 30*, 10382–10387.
Stafford, W. F., III (1992) *Anal. Biochem. 203*, 295–301.
Steiner, R. J., Termonia, Y., & Deltour, J. (1967) *Anal. Chem. 44*, 1906–1909.
Tomski, S. J., & Murphy, R. M. (1992) *Arch. Biochem. Biophys. 294*, 630–638.
Udgaonkar, J. B., & Baldwin, R. L. (1988) *Nature 335*, 694–699.
van Holde, K. E. (1975) in *The Proteins* (Neurath, H., & Hill, R. L., Eds.) pp 225–290, Academic Press, New York.
Volkin, D. B., Tsai, P. K., Dabora, J. M., Gress, J. O., Burke, C. J., Linhardt, R. J., & Middaugh, C. R. (1993) *Arch. Biochem. Biophys. 300*, 30–41.
Wiedlocha, A., Madshus, I. H., Mach, H., Middaugh, C. R., & Olsnes, S. (1992) *EMBO J. 11*, 4835–4842.
Wu, J., Yang, J. T., & Wu, C. C. S. (1992) *Anal. Biochem. 200*, 359–364.
Yutani, K., Ogasahara, K., & Kuwajima, K. (1992) *J. Mol. Biol. 228*, 347–350.
Zerovnik, E., Jerala, R.; Kroon-Zitko, L., Pain, R. H., & Turk, V. (1992) *J. Biol. Chem. 267*, 9041–9046.
Zhu, X., Komiya, H., Chirino, A., Faham, S., Fox, G. M., Arakawa, T., Hsu, B. T., & Rees, D. C. (1991) *Science 251*, 90–93.
Zwanzig, R., Szabo, A., & Bagchi, B. (1992) *Proc. Natl. Acad. Sci. U.S.A. 89*, 20–22.